MODELING OF THE CONJUGATE RADIATION AND CONDUCTION PROBLEM IN A 3D COMPLEX MULTI-BURNER FURNACE

by

Khosro LARI [*] ***and Seyyed Abdolreza GANDJALIKHAN NASSAB***

Department of Mechanical Engineering, Shahid Bahonar University, Kerman, Iran

Radiation is a major component of heat transfer in the modeling of furnaces. In this study, coupled radiative and conductive heat transfer problems are analyzed in complex geometries with inhomogeneous and anisotropic scattering participating media. A three-dimensional model is developed using combination of the discrete ordinates method and blocked-off-region procedure. The finite volume method has been adopted to solve the energy equation and the radiative source term in the energy equation is computed from intensities field. The accuracy of radiative conductive model is verified by comparison with benchmark solutions from the literature. As an example of engineering problems, radiative-conductive heat transfer in a furnace model with gray, inhomogeneous and anisotropic scattering media is numerically studied. The distributions of temperature and heat flux in the furnace are analyzed for different thermoradiative parameters such as conduction-radiation parameter, scattering albedo and anisotropic scattering coefficient. The numerical algorithm described is found to be fast and reliable for studying combined conductive and radiative heat transfer in three-dimensional irregular geometries

Keywords: *three-dimensional complex geometries, radiation, conduction, blocked-off method, discrete ordinates method*

1. Introduction

Growing of energy consumption and generation of combustion pollutants causes the necessity of developing of the thermal performances in the combustion systems. This purpose can be obtained by improving mathematical models to design combustion systems that have enhanced energy efficiency with reduced pollutants production. Radiation heat transfer is an essential mode of heat transfer in high temperatures industrial systems such as combustion chambers and furnaces. So, it is important to develop mathematical models with high strength to analyze thermal radiation especially in case of combustion systems with coupled heat transfer modes and in enclosures with complex geometries [1].

[*] Address of corresponding author: Department of Mechanical Engineering, School of Engineering, Shahid Bahonar University, Jomhoori Eslami blvd., P. O. Box 76175-133, Kerman, IRAN.
Tel.: +98-341-2111763; Fax: +98-341-2120964; E-mail: k.lari@ymail.com

Recently, considerable attention has been paid to the development of accurate and efficient methods for handling the radiation heat transfer. Among other methods, the discrete ordinates method (DOM) has received increasingly more attention because of its capability to join with other algorithms such as common control volume algorithms used in fluid dynamics. The method of discrete ordinates DOM is a straightforward method to solve radiative transfer problems. It offers a good compromise between accuracy and computational requirements. In particular, the DOM was originally formulated by Chandrasekar in 1950 [2], and has been deeply studied by Carlson and Lathrop in 60-70's [3] and by Fiveland and Truelove in the 80's [4, 5].

Among the few earlier works on radiation problems with inhomogeneous participating media, Henson and Malalasekera [6] studied a comparison of the Monte Carlo and the discrete transfer method in 3D inhomogeneous scattering media. Guo and Maruyama [7] developed the REM^2 method to investigate radiative heat transfer in inhomogeneous, non-gray and anisotropically scattering media. The discrete ordinates method has been reformulated to include effects of weak inhomogeneity in 3D mediums by Galinsky [8]. Zorzano et al. [9] considered the atmospheric radiation transfer with discrete ordinates method in plane-parallel problems with strongly non-homogeneous media. Formulation of the FT*n* finite volume method using the blocked-off-region technique in 3-D complex inhomogeneous participating media was presented by Guedri et al. [10].

In order to avoid the complexity of treating non-orthogonal grids, it is suitable to formulate a procedure to model irregular geometries using Cartesian coordinates formulation. The blocked-off method which was previously applied in the computational fluid dynamics (CFD) problems [11] is a procedure that can model complex geometries using Cartesian regular mesh. This method can be used to treat both curved and inclined surfaces. It was firstly used in two-dimensional radiative transfer problems by Chai et al. [12, 13]. They found very promising results for different 2D problems. Coelho et al. [14] used this method with the FVM and the DOM to predict radiative heat transfer in enclosures containing obstacles of very small thickness (baffles). The block-off method is used in the work of Guedri et al. [10] for inhomogeneous gray participating media and Borjini et al. [15] in another work used the same formulation and geometry with non-gray sooting media. Comparison between three types of boundary treatments, the spatial multiblock, blocked-off and embedded boundary has been studied by Byun et al. [16] for different cases of two-dimensional complex enclosures.

Many researchers have studied problems with combined conduction-radiation heat transfer. Tan [17] used the product integration method for solving combined conduction-radiation problem in square enclosure with isothermal walls. The discrete ordinates method found its application in the work of Kim and Baek [18] in the case of coupled radiative and conductive heat transfer in rectangular enclosures. Rousse [19] and Rousse et al. [20] used the Control-Volume Finite Element Method (CVFEM) for the solution of combined mode of heat transfer in two-dimensional cavities. Three dimentional complex enclosures with coupled radiative and conductive heat transfer was studied in the work of Guedri et al. [21] using the finite volume method in gray absorbing-emitting and isotropically scattering medium. They found satisfactory solutions with comparison to reference data. Recently, Amiri et al. [22] analyzed the problem of combined conduction and radiation heat transfer in 2D irregular geometries by using DOM and blocked-off method with both temperature and heat flux boundary conditions. Chaabane et al. [23] proposed a hybrid solver based on the lattice Boltzmann method (LBM) and the Control Volume Finite Element Method (CVFEM) for solving two dimensional transient conduction and radiation heat transfer problems.

Although, there is a fast growth of research activity in this heat transfer area, but to the best of authors' knowledge, the effects of both radiation and conduction heat transfer on three-dimensional irregular enclosures with inhomogeneous and anisotropically scattering media and with the flame effects has not been investigated.

Therefore, in the present study, a three-dimensional blocked-off-region procedure was offered to model combined conductive and radiative heat transfer in multi-burner furnace with complex geometries and inhomogeneous participating media. The energy equation is solved using the finite volume method and the radiative source term in the energy equation is computed from intensities field. The standard solution of discrete ordinates method has been adopted to solve the radiative transfer equation in an absorbing-emitting and anisotropic scattering medium. The radiative conductive model is validated by comparison with the well-documented results in literature. Furthermore, as a case of engineering applications this formulation is applied to analyze the effect of the main thermoradiative parameters on the temperature and radiative flux distributions in a three-dimensional multi-burner furnace with inhomogeneous participating media.

2. Mathematical and numerical formulations

2.1. Energy and radiative transfer equations

The energy equation for coupled radiation–conduction heat transfer of an absorbing, emitting and scattering media under steady state condition with constant thermal conductivity and heat generation is:

$$k\nabla^2 T - \nabla.q_r + \dot{q}''' = 0 \tag{1}$$

where $\dot{q}'''$ (W/m^3) is heat generation per unit volume. To obtain the temperature distribution in the medium by solving Eq. (1), it is necessary to relate $\nabla.q_r$ to the temperature distribution within the medium. One approach is to obtain $\nabla.q_r$ directly by considering the local radiative interaction with a differential volume in the medium. The local divergence of the radiative flux is related to the local intensities by

$$\nabla.q_r = \kappa\left[4\pi I_b(r) - \int_{4\pi} I(r,\Omega)d\Omega\right] \tag{2}$$

To obtain the radiation intensity field and $\nabla.q_r$, it is necessary to solve of the radiative transfer equation (RTE). This equation for an absorbing, emitting and scattering gray medium can be written as in Modest [24],

$$(\Omega.\nabla)I(r,\Omega) = -\beta I(r,\Omega) + \kappa I_b(r) + \frac{\sigma_s}{4\pi}\int_{4\pi} I(r,\Omega')\Phi(\Omega,\Omega')d\Omega' \tag{3}$$

where $I(r,\Omega)$ is the radiation intensity in position r, and in the direction Ω, $I_b(r)$ is the radiation intensity of the blackbody in the position r and at the temperature of the medium, κ and σ_s

are the gray medium absorption and scattering coefficients, respectively, $\beta = (\kappa + \sigma_s)$ is the extinction coefficient, and $\Phi(\Omega, \Omega')$ is the scattering phase function for radiation from incident direction Ω' to scattered direction Ω, and the integration is in the incident direction. For linear-anisotropic scattering, phase function is:

$$\Phi(\Omega, \Omega') = 1 + A_1(\Omega.\Omega') \tag{4}$$

in which $-1 \le A_1 \le 1$ is an asymmetry factor. Values of parameter A_1 are $+1$, 0 or -1 whether scattering is forward, isotropic or backward, respectively.

For diffusely reflecting surfaces, the radiative boundary condition for Eq. (3) is

$$I(r, \Omega) = \varepsilon I_b(r) + \frac{\rho}{\pi} \int_{n.\Omega'<0} I(r, \Omega') |n.\Omega'| d\Omega' \tag{5}$$

where r belongs to the boundary surface and Eq. (7) applies for $n.\Omega > 0$, $I(r, \Omega)$ is the radiation intensity leaving the surface at the boundary condition, ε is the surface emissivity, ρ is the surface reflectivity, and n is the unit vector normal to the boundary surface.

In the method of discrete ordinates, the equation of radiation transfer is substituted by a set of M discrete equations for a finite number of directions Ω_m, and each integral is substituted by a quadrature series of the form,

$$(\Omega_m.\nabla) I(r, \Omega_m) = -\beta I(r, \Omega_m) + \kappa I_b(r) + \frac{\sigma_s}{4\pi} \sum_{k=1}^{M} w_k I(r, \Omega_k) \Phi(\Omega_m, \Omega_k) \tag{6}$$

subject to the boundary conditions

$$I(r, \Omega_m) = \varepsilon I_b(r) + \frac{\rho}{\pi} \sum_{n.\Omega_k<0} w_k I(r, \Omega_k) |n.\Omega_k| \tag{7}$$

where w_k are the quadrature weights. This angular approximation transforms the original equation into a set of coupled differential equations [24].

2.2. Method of solution of radiative-conductive model

To solve the coupled radiation–conduction problem, the equations (1) and (2) are converted to non-dimensional form,

$$\frac{\partial^2 \theta}{\partial X^2} + \frac{\partial^2 \theta}{\partial Y^2} + \frac{\partial^2 \theta}{\partial Z^2} + \dot{Q}''' = S_r \tag{8}$$

$$S_r = \frac{\tau^2 (1-\omega)}{N_{cr}} \left(\theta^4(r) - \frac{1}{4} \sum_{k=1}^{M} w_k \bar{I}(r, \Omega_k) \right) \tag{9}$$

with employing a reference length, L_*, a reference absolute temperature, T_*, and the following dimensionless variables,

$$\theta = \frac{T}{T_*},\ X = \frac{x}{L_*},\ Y = \frac{y}{L_*},\ Z = \frac{z}{L_*},\ \tau = \beta L_*,\ \bar{I} = \frac{I}{\sigma T_*^4},\ N_{cr} = \frac{k\beta}{4\sigma T_*^3},\ Q = \frac{q}{\sigma T_*^4},\ \dot{Q}''' = \frac{\dot{q}''' L_*^2}{kT_*} \quad (10)$$

where N_{cr} is the Conduction-Radiation parameter (the Stark number, Rousse [19]).

The procedure of the numerical calculations starts by assuming that the radiative source term is zero and the energy equation is solved to find the temperature field. The line by line TDMA Algorithm is used to quickly bring the information from all boundaries to the interior. Then the RTE is solved using DOM. The finite volume technique is used to discretize the spatial part of the RTE and an iterative procedure is employed to determine the intensity radiation field. The discretization details and solution procedure can be found in [24]. The employed angular quadrature set is the S_N. Consequently, the radiative source term is calculated and the energy equation is solved including the source term only once for the global iterative process to permit faster convergency.

The iterative process continues until achieving convergence of the intensities and the temperature field. The convergence of the solution was evaluated using a convergence criterion taken as the error in the intensity field in RTE solution and the error in the temperature field for each node p, respectively, by the following criteria:

$$\begin{aligned} error\ \ I &= Max\left|\frac{\bar{I}_p^{\,n} - \bar{I}_p^{\,n-1}}{\bar{I}_p^{\,n}}\right| \le 10^{-6} \\ error\ \ T &= Max\left|\frac{\theta_p^{n} - \theta_p^{n-1}}{\theta_p^{n}}\right| \le 10^{-6} \end{aligned} \quad (11)$$

2.3. The Blocked-off method

Irregular enclosures usually model using body-fitted mesh which grid lines are not necessarily orthogonal to each other. This kind of mesh demands extra complication in computations. In this work a treatment for irregular geometries in Cartesian coordinates has been presented that called the block-off region procedure.

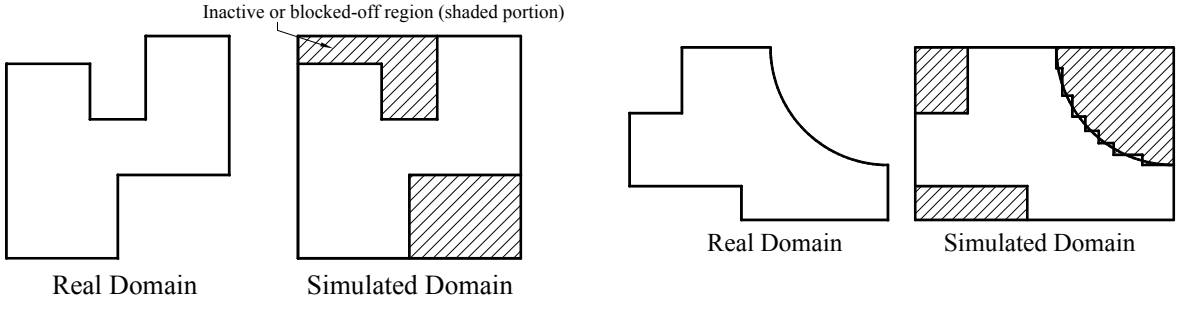

Figure 1. Sample irregular geometries

The philosophy of this procedure consists on drawing nominal domains around given physical domains, so the region is divided into two parts: active and inactive or blocked-off regions. With this method, we can use the same rectangular (cubic in 3D enclosures) algorithms to handle curved or inclined boundaries. Two sample 2D geometries (for better observation) are presented in fig. 1 to show how they are treated to simulate from a rectangular geometry. In these figures, shaded portion is called inactive or blocked-off region. The remaining portion is the active region which is the real domain of interest. Curved boundaries appear to be a stair-stepped mesh as shown in fig. 1(b).

In order to distinguish active region from inactive one in the blocked-off method, an additional source term is introduced [10, 12 and 13],

$$S_{r,bloc} = S_{rC} + S_{rP} I \tag{12}$$

and added to the right part of Eq. (6).

For a given real black boundary, in a cell in the inactive region, the additional source term becomes $(S_{rC}, S_{rP}) = (MI_b, -M)$ (where M is a larger number). This additional source term forces the nodal intensity of the inactive control volumes to $I_p = I_b$. In the active region, the additional source term becomes $(S_{rC}, S_{rP}) = (0, 0)$.

For the case of real gray boundaries, we distinguish between emitted and reflected intensities. In the inactive cells the additional source terms is equal at $(\varepsilon MI_b, -M)$ for the emitted part [10]. Thus, the nodal intensity of the inactive control volumes becomes $I_p = \varepsilon I_b$. The reflected part is added directly into the active region calculation of the control volumes adjacent to the real boundaries (active cell in direct contact with an inactive cell). The additional source terms for the reflected part becomes,

$$(S_{rC}, S_{rP}) = \left(C \frac{\rho}{\pi} \sum_{n.\Omega_k < 0} w_k I(r, \Omega_k) |n.\Omega_k|, 0 \right) \tag{13}$$

where C is a coefficient that is obtained from the discretized formulation of RTE. This coefficient is determined such that the intensity at the real boundaries satisfies Eq. (7).

For the energy equation, the blocked-off-region technique consists on introducing a source term in the discretized energy equation,

$$S_{c,bloc} = S_{cC} + S_{cP} T_p \tag{13}$$

where for all active control volume, the additional source term becomes $(S_{cC}, S_{cP}) = (0, 0)$. But in the inactive region, those coefficients are given by $(S_{cC}, S_{cP}) = (MT_b, -M)$ [21].

3. Validation

To show the validity and the accuracy of the current method, different test problems are analyzed and comparisons are made with the available results in literature.

3.1. Test Problem 1 (The blocked-off method validation)

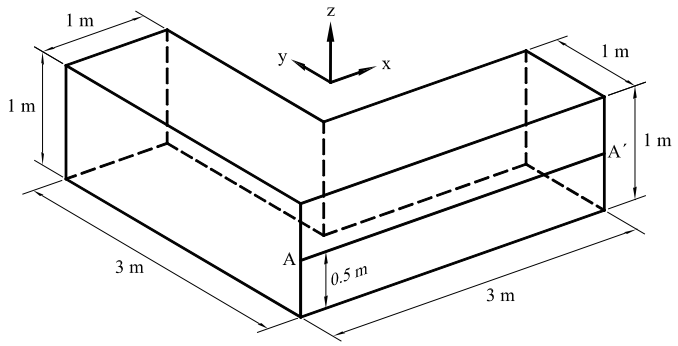

Figure 2. The geometry of test problem 1

For the first test case an L-shaped enclosure is considered containing an emitting-absorbing medium at a temperature of $1000\,\mathrm{K}$ (see fig. 2), where the walls are black at $500\,\mathrm{K}$. The employed grid includes $12\times12\times5$ uniform control volumes, with $8\times8\times5$ control volumes in the block-off region. This test case is investigated in the works of Sakami et al. [25] (a new three-dimensional algorithm based on the discrete-ordinates method and using an S_4 quadrature with the exponential spatial discretization scheme applied to a grid include 2000 tetrahedra) and Joseph et al. [26] (standard discrete ordinates method applied to a non-orthogonal structured grid with the S_4 angular quadrature and the step differencing scheme).

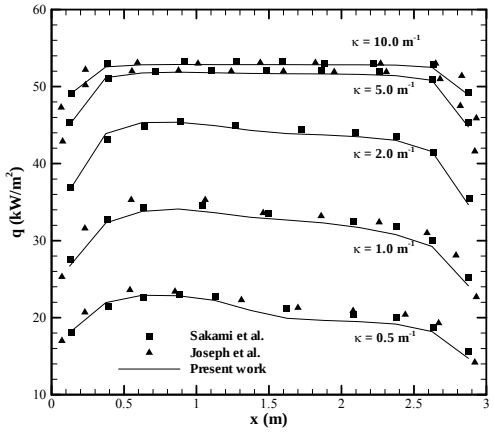

Figure 3. Net heat flux along line AA' of the L-shaped enclosure (Fig. 2), comparison with the results of Sakami et al. and Joseph et al. $(\omega=0,\varepsilon=1.0)$

Effect of the absorption coefficient of the medium on the wall heat flux exited from the AA' line (marked on fig. 2) is displayed in fig. 3. These results were obtained by using of S_4 quadrature with the step scheme. Comparison between the present results with those obtained in Sakami et al. [25] and Joseph et al. [26] shows an appropriate consistency. It can be found from this figure that the effect of the left-hand branch of the L-shaped becomes less important as the absorption coefficient increases.

3.2. Test Problem 2 (Conduction-Radiation validation)

In this section, coupled conduction-radiation problem is analyzed in a three-dimensional rectangular enclosure with participating media. The dimensions of this tested geometry are

$L_x \times L_y \times L_z = 1 \times 10 \times 1\ \mathrm{m}^3$. The bottom wall $(z = 0)$ is hot at dimensionless temperature $\theta = 1$ and other walls are cold at dimensionless temperature $\theta = 0.5$. The media in cavity is gray and the boundaries are black surfaces. The medium is further assumed to absorb and emit radiation with $\kappa = 1\,\mathrm{m}^{-1}$, but not scatter radiant energy, $\omega = 0$. This test problem has been solved in the work of Guedri et al. [21]. They used finite volume method to model combined conductive and radiative heat transfer. In the present work $21 \times 21 \times 11$ control volumes and S_4 angular quadrature is used.

The effect of conduction-radiation parameter N_{cr} on the dimensionless temperature at the symmetry line $(x = L_x/2,\ y = L_y/2)$ is presented in fig. 4. A finite volume solution is also given for the case of pure conductive heat transfer. As N_{cr} decreases, radiation plays a more significant role than conduction. Therefore, as N_{cr} decreases, a steeper temperature gradient is formed at both end walls (right and left surfaces) and the medium temperature inside increases as shown in fig. 4. The present results show comparable accuracy with those presented by Guedri et al. [21] and the finite element method solutions in the work of Razzaque et al. [27].

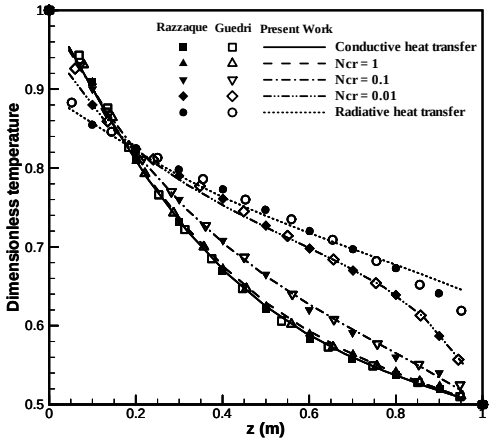

Figure 4. Dimensionless temperature profiles at line $x = L_x/2,\ y = L_y/2$ for various conduction-radiation parameters N_{cr}. $(\omega = 0, \tau = 1)$

4. Results and discussion

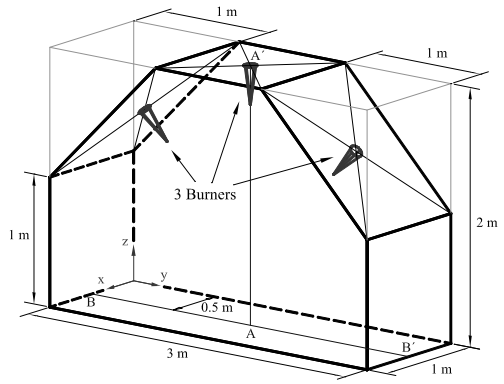

Figure 5. Schematic of a 3D furnace enclosure with simulated domain

In this section, as an example of an application of engineering interest, the block-off region procedure is applied to a three-dimensional furnace. Figure 5 shows the schematic and dimensions of this 3D furnace enclosure with its simulated domain. The furnace has two incline boundary planes on

top-right and top-left and three burners that are sited on the middle of these two incline planes and horizontal top plane as shown in fig. 5. Each burner exit is simulated with a cone that radius of its base is equal to $5\,\mathrm{cm}$ and height equal to $30\,\mathrm{cm}$.

It should be mentioned that this model is not realistic. We have adopted this model to assess the applicability of the present method in analyzing radiative transfer in complex configurations with inhomogeneous and linear-anisotropic scattering media. The calculations have been carried out for several cases with combined conduction-radiation situation to investigate the effects of conduction-radiation parameter N_{cr} and scattering albedo ω on thermal behavior of the system. Also, anisotropic scattering effects has been analyzed by using the different values of the scattering phase function coefficient A_1.

The medium is considered as gray and all furnace walls are diffuse with emissivity of 0.8. The temperature of walls is $T = 600\,\mathrm{K}$ which is also considered as the reference temperature. Since the present paper has been focused on combined radiative and conductive heat transfer modeling, the combustion process at the each burner is modeled as a uniform heat generation zone that takes place in flame cone areas shown in fig. 5. The immediate advantage of this approach is that it doesn't need to render fully detailed modeling of the combustion process.

The media in furnace enclosure, especially because of combustion process, consists of different gases and the temperature of the domain has intensive variation that makes variable absorption coefficient at the different points of the domain. So, considering homogeneous enclosure makes significant errors in the calculations. Therefore in this study, inhomogeneous participating media with temperature dependent absorption coefficients for the furnace enclosure is considered.

In order to achieve this purpose, the data of Coelho et al. [14] work is used. In their work, radiation analysis in a combustion chamber of a utility boiler was investigated with three fixed different temperatures and absorption coefficients for various areas of enclosure. Because, in our work combined radiation and conduction heat transfer is analyzed and the temperature of furnace enclosure is not fixed, so a continuous distribution of absorption coefficient versus temperature is needed. Therefore, as shown in fig. 6, an exponential interpolation of the data of Coelho et al. work is obtained.

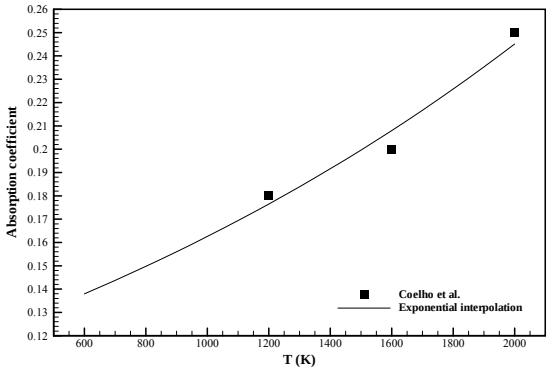

Figure 6. Absorption coefficient vs. temperature obtained using exponential interpolation on the data of Coelho et al. work

For using these temperature dependent absorption coefficients, first an initial solution with averaged absorption coefficient for entire computation domain is achieved. Then absorption coefficients of the domain are corrected based on the obtained temperature field and another solution is performed. This iterative process continues until achieving convergence.

To check whether the grid resolution used is adequate, a grid independent study is carried out for the furnace with $N_{cr}=0.01$ and $\omega=0$ at four spatial grid sizes, i.e., $11\times31\times21$, $15\times45\times31$, $21\times61\times41$ and $31\times91\times61$. The calculated thermal energy out going from the bottom wall of the furnace for the four grid sizes are 315.06 W, 235.488 W, 205.681 W and 199.475 W, respectively. The percentage of difference between the first and second grid values is 25.2%, between the second and third grid values is 12.6% and between the third and forth grid values is 3.0%. Using these results, a spatial grid size of $21\times61\times41$ is chosen as optimum for the present problem. For the angular resolution, S_{12} angular quadrature is selected. Grid independence study shows that the results did not fully achieve grid independence. However, it has been checked that further refinement of the grids does not affect the qualitative conclusions of this study but greatly increases the computing time [28].

In the first test case, the medium is considered to be non-scattering. Figure 7 shows the dimensionless temperature along the *z*-direction at the line AA' of the furnace enclosure (marked on fig. 5) for various values of the conduction-radiation parameter N_{cr} while other parameters are fixed. For better observation, only the upper half of the line AA' has been shown $(1\le z\le 2)$. It is obvious that when N_{cr} increases the conductive heat transfer mode becomes dominant until it reaches infinity that in this point, the energy equation will transform into purely conduction heat transfer. As shown in fig. 7, when N_{cr} is unity, the temperature profile is not greatly affected by radiation when compared to the case of pure conduction. This suggests that the magnitude of the conduction-radiation parameter should be less than unity to require a radiation heat transfer calculation $(N_{cr}\le 1)$. In an opposing manner, when N_{cr} decreases, radiative heat transfer becomes predominant. It is seen from this figure that the maximum temperature is occurred in the flame area.

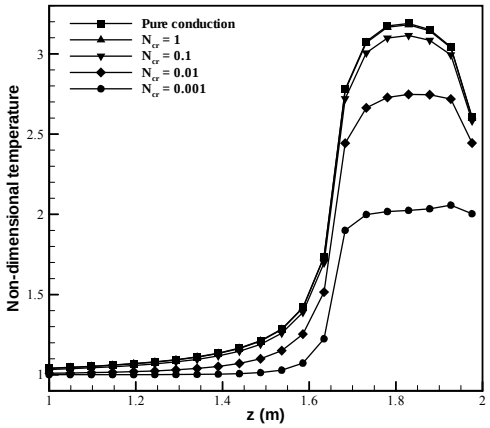

Figure 7. Dimensionless temperature profiles at line AA' for various conduction-radiation parameters N_{cr}. $(\omega=0)$

In order to better studying the effect of conduction-radiation parameter N_{cr} on temperature profiles, isothermal contours at the plane $x=L_x/2$ for four various N_{cr} have been shown in fig. 8. The effect of three burners' flames on temperature field has clearly appeared in this figure. It can be seen that when N_{cr} gradually decreases and radiative heat transfer becomes dominant mode, isotherms concentrate around the flames that cause sharp slope in the temperature profiles.

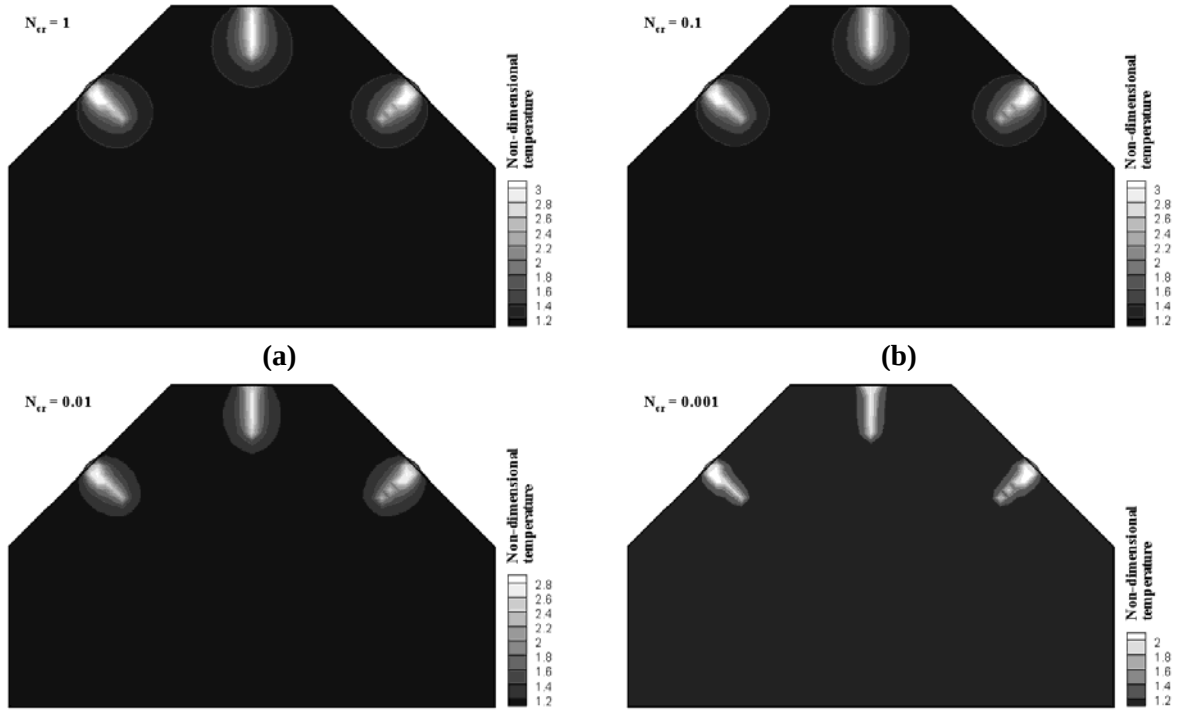

Figure 8. Isotherms at the plane $x = L_x / 2$ for various conduction-radiation parameters N_{cr}. $(\omega = 0)$

The non-dimensional total heat flux and the fractional radiative heat flux along the line BB' of the furnace enclosure (marked on fig. 5) for different values of N_{cr} are shown in fig. 9. The total heat flux is the summation of radiative heat flux and conductive heat flux. Also, the fractional radiative heat flux is the ratio of radiative heat flux to the total heat flux. Because the furnace is symmetric along the plane $y = L_y / 2$, the results is shown for half of line BB' $(0 \le y \le 1.5)$. Figure 9(a) shows that the total flux becomes clearly much higher as N_{cr} increases and more uniform as N_{cr} decreases. According to fig. 9(b), the fractional radiative heat flux is seen to increase when N_{cr} decreases. Figure 9(b) truly reveals earlier described sentence that when N_{cr} decreases, radiative heat transfer becomes predominant.

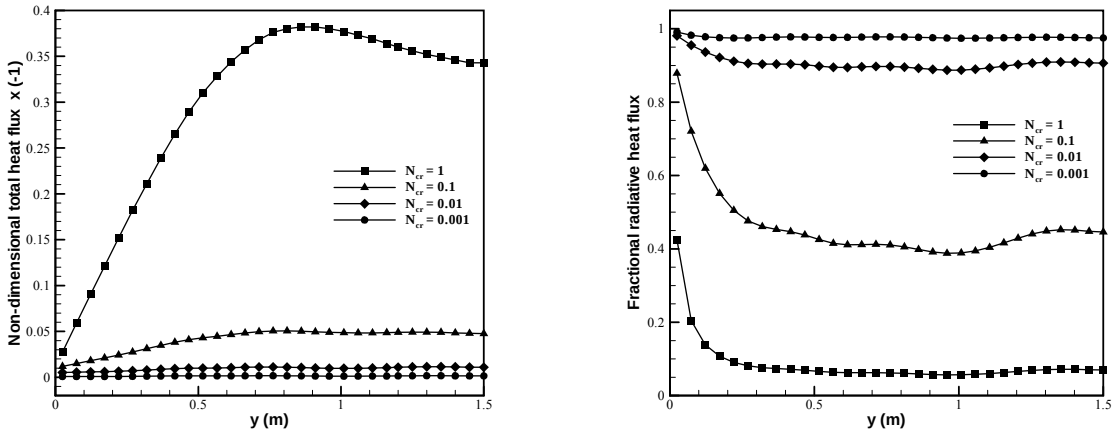

Figure 9. (a) Non-dimensional total heat flux; and (b) fractional radiative heat flux at line BB' for various conduction-radiation parameters N_{cr}. $(\omega = 0)$

Again, for better observing, the non-dimensional total heat flux contours at the front plane $(x = L_x)$ and bottom plane $(z = 0)$ for various conduction-radiation parameter N_{cr} are shown in Figs. 10 and 11, respectively. It is seen from Fig. 10 that when N_{cr} decreases and radiative heat transfer becomes dominant, heat flux contours concentrate around the flames of burners and disturbance in heat flux distribution progressively grows.

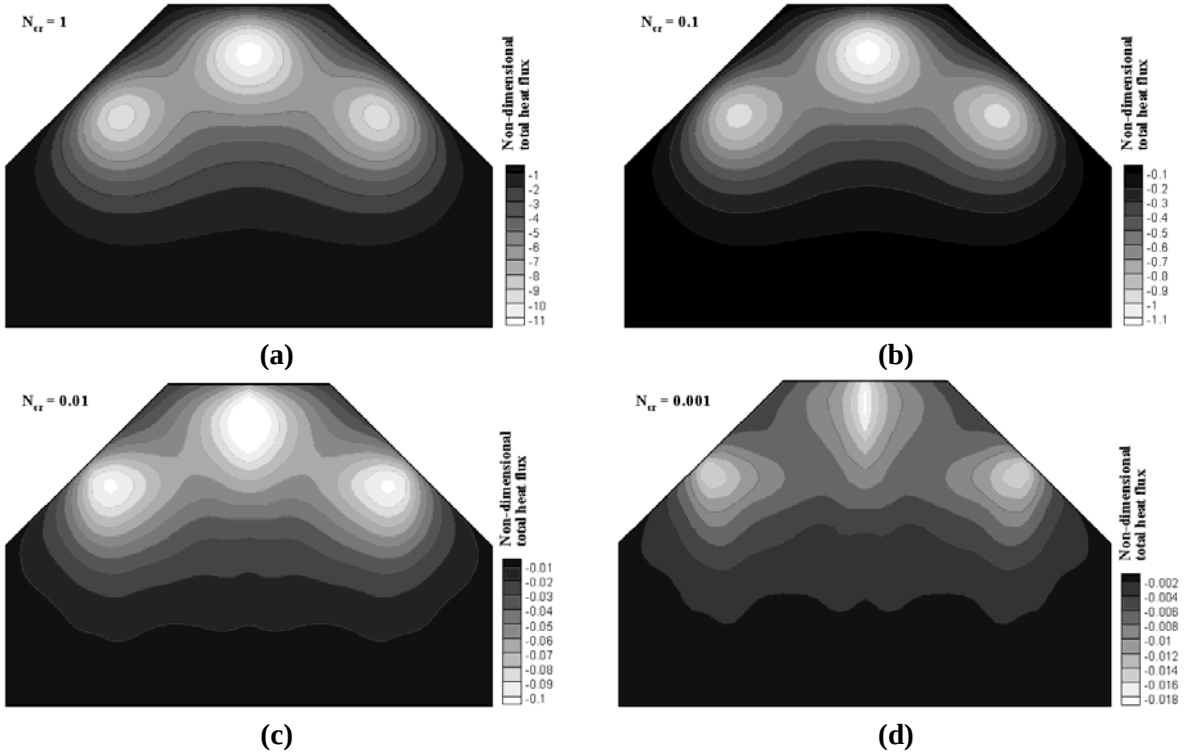

Figure 10. Non-dimensional total heat flux contours at the front plane for various conduction-radiation parameters N_{cr}. $(\omega = 0)$

This disturbance is better seen in fig. 11. In this figure is also observed that when radiation becomes dominant (small N_{cr}), radiation intensity that is reflected from other furnace walls causes multiple projections of flames on bottom plane. For example, it is seen from fig. 11(d) that when $N_{cr} = 0.001$ any burners have four projections on bottom plane.

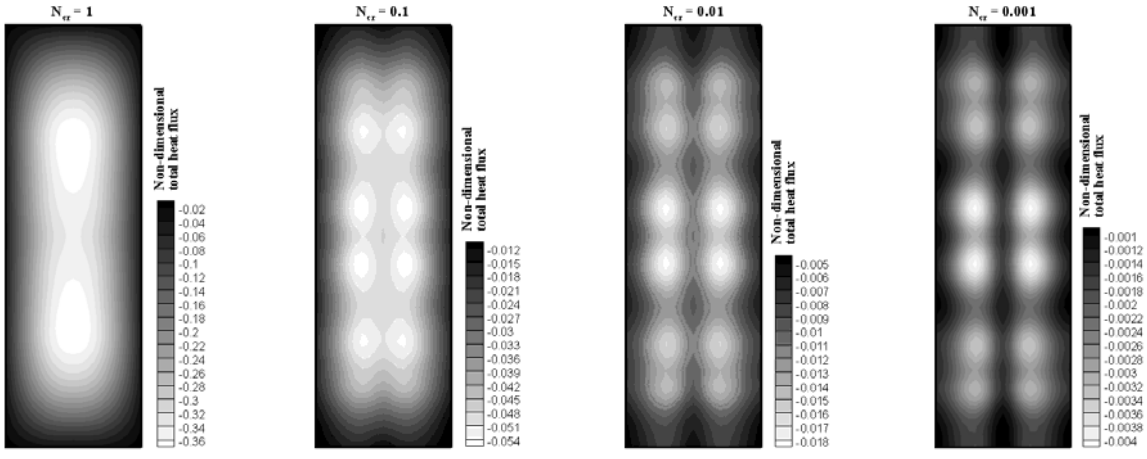

Figure 11. Non-dimensional total heat flux contours at the bottom plane for various conduction-radiation parameters N_{cr}. $(\omega = 0)$

Figure 12 shows the dimensionless total flux and the fractional radiative heat flux at the line BB' for various scattering albedo values with $N_{cr} = 0.01$ and isotropic scattering $(A_1 = 0)$. According to fig. 12(a) it is seen that the dimensionless total heat flux decreases when ω increases. Such event occurs for the fractional radiative heat flux (fig. 12(b)).

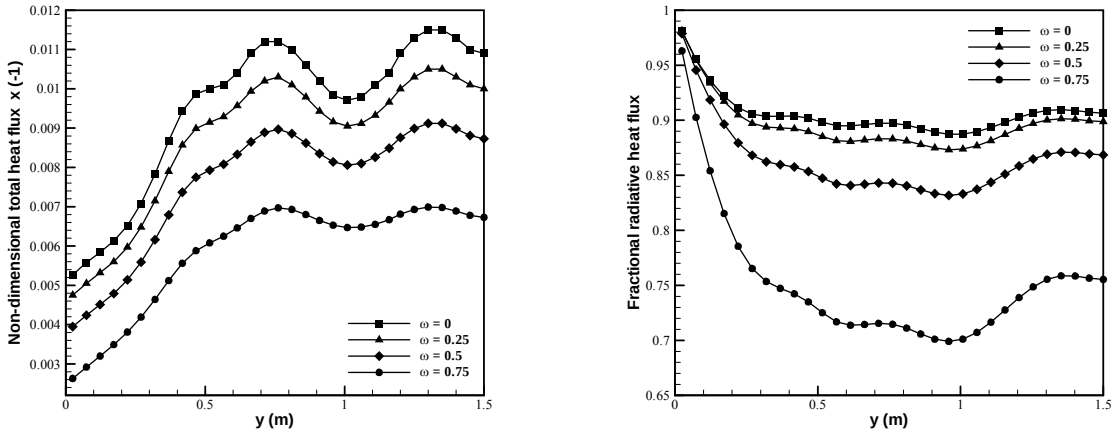

(a) **(b)**

Figure 12. (a) Non-dimensional total heat flux; and (b) fractional radiative heat flux at line BB' for various scattering albedos ω. $(N_{cr} = 0.01, A_1 = 0)$

In the following, we fixed the conduction-radiation parameter at $N_{cr} = 0.01$ and the scattering albedo at $\omega = 0.5$. The dimensionless total heat flux and the fractional radiative heat flux along the line BB' are shown in fig. 13 for various values of the scattering phase function coefficient A_1 to analysis the effect of linear-anisotropic scattering. It can be seen from this figure that the total heat flux and the fractional radiative heat flux are higher in forward scattering situation and lower in backward scattering. But it is obvious that in general they are approximately insensitive to this parameter. So, it can be concluded that linear-anisotropic scattering doesn't have much effect on thermal behavior of system.

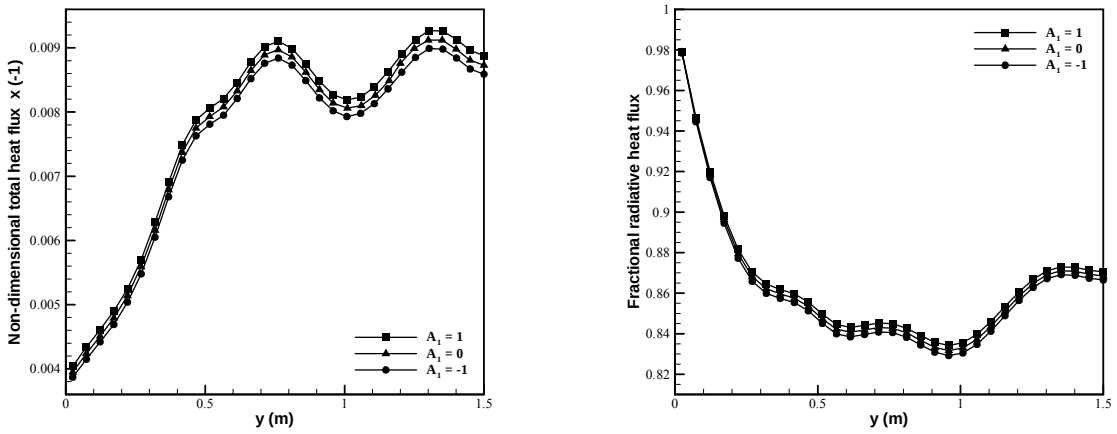

(a) **(b)**

Figure 13. (a) Non-dimensional total heat flux; and (b) fractional radiative heat flux at line BB' for various scattering phase function coefficient A_1. $(N_{cr} = 0.01, \omega = 0.5)$

5. Conclusions

An original 3D combination of the discrete ordinates method and the blocked-off-region technique was developed for analysis of combined conduction-radiation heat transfer problems. The blocked-off method that is used in this work is simple and has the major advantage of using the same rectangular (cubic in 3D enclosures) algorithm for all types of geometries and can be utilized coupled with common control volume algorithms used in fluid dynamics.

In the first part of this work, this approach was applied to three-dimensional complex enclosures with diffuse reflective surfaces and containing gray absorbing-emitting and scattering medium. Results show that both wall heat flux and temperature distributions predictions are satisfactory when compared to benchmarked results. This consistency confirms that this method is a good general way for studying combined conductive-radiative heat transfer in three-dimensional irregular geometries. It is evident that for curved or inclined boundaries, a fine or a non-uniform grid is needed.

In the second part, a multi-burner furnace enclosure as an engineering case study of combined conductive-radiative heat transfer is analyzed with inhomogeneous and anisotropic scattering media. Three burners' flames of the furnace are modeled as uniform heat generation zones. The effects of various influencing parameters such as conduction-radiation parameter, scattering albedo and anisotropic scattering coefficient on the temperature and wall heat flux distributions are investigated. It is evidenced from the results that the magnitude of the ratio of the radiant heat transfer to the conduction heat transfer should be at least unity to require a radiation heat transfer calculation $(N_{cr} \le 1)$. Also, when the radiation heat transfer becomes dominant disturbance is clearly seen in the heat flux contours.

According to the results, this method is strongly recommended and it's formulation with the blocked-off-region procedure develops an accurate and simple numerical tool to deal with 3D radiative transfer in complex geometries with inhomogeneous media.

Nomenclature

A_1 – scattering phase function coefficient, [–]
I – radiation intensity, [$W/m^2.sr$]
$\bar{I}$ – dimensionless radiation intensity, [–]
k – thermal conductivity, [W/m.K]
L – length, [m]
M – number of discrete directions, [–]
n – unit vector normal to the surface, [–]
N_{cr} – conduction-radiation parameter ($=k\beta/4\sigma T^3$), [–]
q – heat flux, [W/m^2]
Q – dimensionless heat flux, [–]
$\dot{q}'''$ – heat source per unit volume, [W/m^3]
$\dot{Q}'''$ – dimensionless heat source per unit volume, [–]
r – position vector, [m]
S – source term, [W/m^3]
T – temperature, [K]
w – quadrature weights, [–]
x, y, z – coordinate, [m]
X, Y, Z – dimensionless coordinate, [–]

Greek symbols

β – extinction coefficient, [m^{-1}]
ε – emissivity of a surface, [–]
θ – dimensionless temperature, [–]
κ – absorption coefficient, [m^{-1}]
ρ – reflectivity of the surface, [–]
σ – Stefan-Boltzmann constant ($=5.670\times10^{-8}$), [$Wm^{-2}K^{-4}$]

σ_s – scattering coefficient, [m^{-1}]
τ – optical thickness ($=\beta L$), [–]
Φ – scattering phase function, [–]
ω – scattering albedo, [–]
Ω – direction vector, [–]

Subscripts

* – reference quantity
b – black body
m – discrete direction
p – nodal point
r – radiation

Superscripts

′ – incoming direction
n – iteration step

References

[1] Baburic, M., Raulot, A., Duic, N., Implementation of discrete transfer radiation method into swift computational fluid dinamics code, *Thermal Science*, 8 (2004), 1, pp. 19-28

[2] Chandrasekhar, S., Radiative transfer, Clarendon Press, Oxford, UK, 1950

[3] Carlson, B. G., Lathrop, K. D., in: *Computing methods of reactor physics*, Gordon & Breach, New York, USA, 1968, pp. 165–266

[4] Fiveland, W. A., Three-dimensional radiative heat transfer solutions by the discrete-ordinates method, *Journal of Thermophysics*, 2 (1998), pp. 309-316

[5] Truelove, J. S., Three-dimensional radiation in absorbing-emitting-scattering in using the discrete-ordinates approximation, *Journal of Quantitative Spectroscopy & Radiative Transfer*, 39 (1988), pp. 27-31

[6] Henson, J. C., Malalasekera, W. M. G., Comparison of the discrete transfer and Monte Carlo methods for radiative heat transfer in three-dimensional nonhomogenious scattering media, *Numerical Heat Transfer—Part A*, 32 (1997), pp. 19–36

[7] Guo, Z., Maruyama, S., Radiative heat transfer in inhomogeneous, nongray, and anisotropically scattering media, *International Journal of Heat and Mass Transfer*, 43 (2000), pp. 2325–2336

[8] Galinsky, V. L., 3D Radiative Transfer in Weakly Inhomogeneous Medium. Part II: Discrete Ordinate Method and Effective Algorithm for Its Inversion, *Journal of the Atmospheric Sciences*, 57 (2000), pp. 1635-1645

[9] Zorzano, M. P., Mancho, A. M., Vazquez, L., Numerical integration of the discrete-ordinate radiative transfer equation in strongly non-homogeneous media, *Applied Mathematics and Computation*, 164 (2005), pp. 263-274

[10] Guedri, K., Borjini, M. N., Mechi, R., Said, R., Formulation and testing of the FT*n* finite volume method for radiation in 3-D complex inhomogeneous participating media, *Journal of Quantitative Spectroscopy & Radiative Transfer*, 98 (2006), pp. 425-445

[11] Patankar, S. V., Numerical heat transfer and fluid flow, Hemisphere, Washington, D. C., 1980

[12] Chai, J. C., Lee, H. S., Patankar, S. V., Treatment of irregular geometries using a Cartesian-coordinates-based discrete-ordinates-method, *Radiative Heat Transfer—Theory and Application*, 244 (1993), pp. 49-54

[13] Chai, J. C., Lee, H. S., Patankar, S. V., Treatment of irregular geometries using a Cartesian coordinates finite volume radiation heat transfer procedure, *Numerical Heat Transfer—Part B*, 26 (1994), pp. 225–235

[14] Coelho, P. J., Goncalves, J. M., Carvalho, M. G., Modelling of radiative heat transfer in enclosures with obstacles, *International Journal of Heat and Mass Transfer*, 41 (1998), pp. 745-756

[15] Borjini, M. N., Guedri, K., Said, R., Modeling of radiative heat transfer in 3D complex boiler with non-gray sooting media, *Journal of Quantitative Spectroscopy & Radiative Transfer*, 105 (2007), pp. 167-179

[16] Byun, D. Y., Baek, S. W., Kim, M. Y., Investigation of radiative heat transfer in complex geometries using blocked-off, multiblock, and embedded boundary treatments, *Numerical Heat Transfer—Part A*, 43 (2003), pp. 807-825

[17] Tan, Z., Combined radiative and conductive transfer in two-dimensional emitting, absorbing, and an-isotropic scattering square media, *International Communications in Heat and Mass Transfer*, 16 (1989), pp. 391-401

[18] Kim, T. Y., Baek, S. W., Analysis of combined conductive and radiative heat transfer in a two-dimensional rectangular enclosure using the discrete ordinates method, *International Journal of Heat and Mass Transfer*, 34 (1991), pp. 2265-2273

[19] Rousse, D. R., Numerical predictions of two-dimensional conduction, convection, and radiation heat transfer— I. Formulation, *International Journal of Thermal Sciences*, 39 (2000), pp. 315-331

[20] Rousse, D. R., Gautier, G., Sacadura, J. F., Numerical predictions of two-dimensional conduction, convection and radiation heat transfer— II. Validation, *International Journal of Thermal Sciences*, 39 (2000), pp. 332-353

[21] Guedri, K., Borjini, M. N., Farhat, H., Modelization of combined radiative and conductive heat transfer in three-dimensional complex enclosures, *International Journal for Numerical Methods in Heat & Fluid Flow*, 15 (2005), 3, pp. 257-276

[22] Amiri, H., Mansouri, S. H., Safavinejad, A., Combined conductive and radiative heat transfer in an anisotropic scattering participating medium with irregular geometries, *International Journal of Thermal Sciences*, 49 (2010), pp. 492-503

[23] Chaabane, R., Askri, F., Nasrallah, S. B., A new hybrid algorithm for solving transient combined conduction radiation heat transfer problems, *Thermal Science*, Online-First Issue 00(2011), pp. 15-15

[24] Modest, M. F., Radiative heat transfer, 2nd ed., Academic Press, San Diego, USA, 2003

[25] Sakami, M., Charette, A., Dez, V. L., Radiative heat transfer in three-dimensional enclosures of complex geometry by using the discrete-ordinates method, *Journal of Quantitative Spectroscopy & Radiative Transfer*, 59 (1998), pp. 117-136

[26] Joseph, D., Coelho, P. J., Cuenot, B., Hafi, M. E., Application of the discrete ordinates method to grey media in complex geometries using unstructured meshes, *Proceedings*, Eurotherm73 on Computational Thermal Radiation in Participating Media, Belgium, April 15-17, 2003

[27] Razzaque, M. M., Howell, J. R., Klein, D. E., Coupled radiative and conductive heat transfer in a two-dimensional rectangular enclosure with gray participating media using finite element-method, *ASME Journal of Heat Transfer*, 106 (1984), pp. 613-619

[28] Bindar, Y., Experimental and numerical investigations of a multiburner furnace operated with various heat transfer boundary conditions, Ph. D. thesis, Queen's University, Canada, 1996